Journal of Engineering Physics and Thermophysics, Vol. 72, No. 3, 1999

NATURAL CONVECTION OF THE EARTH LIQUID CORE IN THE PRESENCE OF INTERNAL HEAT SOURCES

S. V. Solov'ev

UDC 536.25

Results of natural-convection heat transfer in the earth liquid core in the presence of internal sources are presented. Consideration is given to boundary conditions of the I, II, and III kind for the temperature. The effect of internal heat sources on the hydrodynamics and heat transfer of the core is studied.

The modern theory of the geomagnetic field assumes that continuous migration of substance takes place in the earth liquid core [1]. At present, there is no doubt that thermal convection in the earth core is the very reason that causes the formation of the geomagnetic field [2]. The theory of the geomagnetic field has acquired the name geomagnetic dynamo (GD). Mathematical interpretation of the theory of vortical motion in the core and the appearance of induced currents in it is extremely difficult and has not been solved as yet [1]. Therefore, the theory of GD is being developed mainly by studying kinematic models where the velocity of the liquid flow is taken to be set and only the magnetic field is determined [3]. This approach can be compared with the electrodynamics of weak fields [3]. By virtue of this the study of the hydrodynamics of the earth liquid core with natural-convection heat transfer without regard for magnetic forces is of independent interest.

With the aforesaid in mind, in the present paper we study natural-convection heat transfer in the presence of internal heat sources in the earth liquid core, which is considered to be a dielectric non-Newtonian fluid. The Boussinesq approximation is used. Free-fall acceleration is directed toward the core center. The liquid core is considered to be a spherical layer between the inner solid core of the earth and the boundary zone of the mantle with a liquid core [4].

In the present paper problems of the convective stability of a liquid in a spherical cavity were not analyzed because this problem represents a separate study. Fundamentally this problem was studied in [5-9].

The mathematical model of natural-convection heat transfer in the earth liquid core in a spherical system of coordinates with account for the symmetry along the longitude (the Coriolis force is disregarded) is described by the following dimensionless equations:

$$\frac{1}{\mathrm{Sh}}\frac{\partial \vartheta}{\partial \tau} + (\mathbf{V}\nabla)\,\vartheta = \frac{1}{\mathrm{Pe}}\Delta\vartheta + \frac{Q_v}{\mathrm{Pe}}, \tag{1}$$

$$\frac{1}{\mathrm{Sh}}\frac{\partial \mathbf{V}}{\partial \tau} + (\mathbf{V}\nabla)\,\mathbf{V} = -\,\mathrm{Eu}\,\nabla P + \frac{1}{\mathrm{Re}}\Delta\mathbf{V} + \gamma\frac{\mathrm{Gr}}{\mathrm{Re}^2}\vartheta, \tag{2}$$

$$\mathrm{div}\,\mathbf{V} = 0. \tag{3}$$

The geometry of the computational region is given in Fig. 1.

The following notation is used in system (1)-(3): γ is a unit vector directed to the center of the earth; ϑ, $\mathbf{V} = V/u_0$, $\tau = t/t_0$ are the dimensionless temperature, velocity, and time; $\mathrm{Eu} = P_0/\rho_0 u_0^2$ is the Euler number; Re

Khabarovsk State Technical University, Russia. Translated from Inzhenerno-Fizicheskii Zhurnal, Vol. 72, No. 3, pp. 533-544, May-June, 1999. Original article submitted January 28, 1998; revision submitted September 22, 1998.

1062-0125/99/7203-0511$22.00

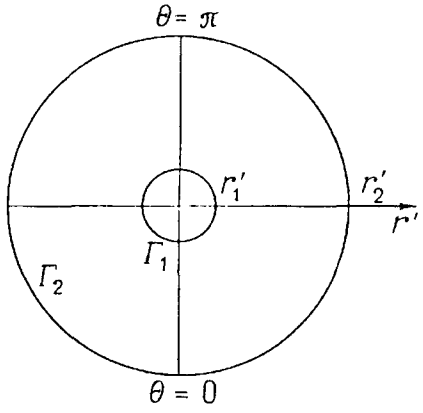

Fig. 1. Computational region.

$= u_0 r_1'/\nu$ is the Reynolds number; $\mathrm{Pe} = u_0 r_1'/a$ is the Peclet number; $\mathrm{Sh} = u_0 t_0/r_1'$ is the Strouhal number; Gr, Q_v are the Grashof number and the dimensionless internal heat source; $r = r'/r_1'$ is the dimensionless radius; r', r_1' are the dimensional current radius and the radius of the inner sphere.

Problem (1)-(3) was solved in the variables of temperature-vortex-stream function. For this purpose the operation rot was applied to both parts of Eq. (2):

$$\frac{1}{\mathrm{Sh}}\,\mathrm{rot}\,\frac{\partial \mathbf{V}}{\partial \tau} + \mathrm{rot}\,(\mathbf{V}\nabla)\,\mathbf{V} = -\,\mathrm{Eu}\,\mathrm{rot}\,\nabla P + \frac{1}{\mathrm{Re}}\,\mathrm{rot}\,\Delta \mathbf{V} + \frac{\mathrm{Gr}}{\mathrm{Re}^2}\,\mathrm{rot}\,\gamma\vartheta\,. \tag{4}$$

If new variables – vortex strength $\mathbf{W} = \mathrm{rot}\,\mathbf{V}$ and stream function Ψ – are introduced:

$$V_r = \frac{1}{r^2 \sin\theta}\,\frac{\partial \Psi}{\partial \theta}\,,\quad V_\theta = -\,\frac{1}{r \sin\theta}\,\frac{\partial \Psi}{\partial r}\,,$$

then in the new variables the system of equations (1-(3) acquires the following form:

$$\frac{1}{\mathrm{Sh}}\,\frac{\partial \vartheta}{\partial \tau} + \frac{1}{r^2 \sin\theta}\left(\frac{\partial \Psi}{\partial \theta}\,\frac{\partial \vartheta}{\partial r} - \frac{\partial \Psi}{\partial r}\,\frac{\partial \vartheta}{\partial \theta}\right) =$$

$$= \frac{1}{\mathrm{Pe}}\left(\frac{\partial^2 \vartheta}{\partial r^2} + \frac{2}{r}\,\frac{\partial \vartheta}{\partial r} + \frac{1}{r^2}\,\frac{\partial^2 \vartheta}{\partial \theta^2} + \frac{\mathrm{ctan}\,\theta}{r^2}\,\frac{\partial \vartheta}{\partial \theta} + Q_v\right), \tag{5}$$

$$\frac{1}{\mathrm{Sh}}\,\frac{\partial \omega}{\partial \tau} + \frac{1}{r^2 \sin\theta}\left[\frac{\partial \Psi}{\partial \theta}\,\frac{\partial \omega}{\partial r} - \frac{\partial \Psi}{\partial r}\,\frac{\partial \omega}{\partial \theta} - \frac{\omega}{r}\,\frac{\partial \Psi}{\partial \theta} + \omega\,\mathrm{ctan}\,\theta\,\frac{\partial \Psi}{\partial r}\right] =$$

$$= \frac{1}{\mathrm{Re}}\left[\frac{\partial^2 \omega}{\partial r^2} + \frac{2}{r}\,\frac{\partial \omega}{\partial r} + \frac{1}{r^2}\,\frac{\partial^2 \omega}{\partial \theta^2} + \frac{\mathrm{ctan}\,\theta}{r^2}\,\frac{\partial \omega}{\partial \theta} - \frac{\omega}{r^2 \sin^2\theta}\right] - \frac{\mathrm{Gr}}{\mathrm{Re}^2}\,\frac{1}{r}\,\frac{\partial \vartheta}{\partial \theta}\,, \tag{6}$$

$$\frac{\partial^2 \Psi}{\partial r^2} + \frac{1}{r^2}\,\frac{\partial^2 \Psi}{\partial \theta^2} - \frac{\mathrm{ctan}\,\theta}{r^2}\,\frac{\partial \Psi}{\partial \theta} = -\,\omega\, r \sin\theta\,. \tag{7}$$

Here ω is the component of the vector of vortex strength along the longitude φ.

To solve boundary-value problem (5)-(7), zero values of the stream function, the vortex strength, and the temperature or a stationary temperature distribution (with and without a heat source) for the case of pure heat conduction were assigned as initial conditions.

In the present paper boundary conditions of the I, II, and III kind were considered.

Boundary conditions of the I kind:

$$\vartheta|_{\Gamma_1} = 1\,,\quad \vartheta|_{\Gamma_2} = 0\,.$$

Here $\vartheta = (T - T_2)/(T_1 - T_2)$; $\mathrm{Gr} = g\beta(T_1 - T_2)r_1'^3/\nu^2$; $Q_v = q_v r_1'^2/\lambda(T_1 - T_2)$, where λ is the coefficient of thermal conductivity of the earth core; q_v is the internal heat source.

Boundary conditions of the II kind. A heat source q is assigned by the Fourier law on the inner boundary of the core, and the temperature is prescribed on the outer boundary (or conversely):

$$-\left.\frac{\partial\vartheta}{\partial n}\right|_{\Gamma_1} = 1\,,\quad \vartheta|_{\Gamma_2} = 0\,.$$

Here $\vartheta = (T - T_2)\lambda/(qr_1')$; $\mathrm{Gr} = g\beta q r_1'^4/\nu^2\lambda$; $Q_v = q_v r_1'/q$.

Boundary conditions of the III kind. At the boundaries of the core heat transfer occurs according to the Newton–Richman law

$$\mathrm{Bi}_1\vartheta|_{\Gamma_1} = \left.\frac{\partial\vartheta}{\partial n}\right|_{\Gamma_1}\,,\quad \left.\frac{\partial\vartheta}{\partial n}\right|_{\Gamma_2} = \mathrm{Bi}_2\,(1 - \vartheta_{\Gamma_2})\,.$$

Here Bi_1, Bi_2 are the known Biot numbers

$$\mathrm{Bi}_k = \frac{\alpha_k r_1'}{\lambda}\,,\quad k = 1, 2\,;$$

$$\vartheta = \frac{T_{\mathrm{liq1}} - T}{T_{\mathrm{liq1}} - T_{\mathrm{liq2}}}\,;\quad \mathrm{Gr} = -\frac{g\beta r_1'^3\,(T_{\mathrm{liq1}} - T_{\mathrm{liq2}})}{\nu^2}\,;\quad Q_v = -\frac{q_v r_1'^2}{\lambda\,(T_{\mathrm{liq1}} - T_{\mathrm{liq2}})}\,;$$

T_{liq1}, T_{liq2} are the known dimensional temperatures of the liquid that washes the core boundary Γ_1 (from inside) and Γ_2 (from outside), respectively; α_1, α_2 are the coefficients of heat transfer from the side of the liquid that washes the boundaries Γ_1 and Γ_2, respectively.

It should be noted that a combination of the boundary conditions for temperature is possible.

For the equation of energy on the axis of symmetry the derivative of temperature became zero:

$$\left.\frac{\partial\vartheta}{\partial\theta}\right|_{\theta=0,\pi} = 0\,.$$

The boundary conditions for the stream function are the following:

$$\Psi|_{\Gamma_{1,2}} = \left.\frac{\partial\Psi}{\partial r}\right|_{\Gamma_{1,2}} = 0\,;\quad \Psi|_{\theta=0,\pi} = \left.\frac{\partial^2\Psi}{\partial\theta^2}\right|_{\theta=0,\pi} = 0\,.$$

The boundary conditions for the vortex strength on the walls suggest a linear variation of ω along the normal. The boundary condition for ω on the axis of symmetry is taken from [10].

To evaluate the intensity of natural convection in the earth liquid core the local and averaged Nusselt numbers were calculated.

The local Nusselt numbers on the surfaces of the inner and outer spheres were calculated by the formulas

$$\mathrm{Nu}_1 = -\left.\frac{\partial\vartheta}{\partial r}\right|_{\Gamma_1}\,,\quad \mathrm{Nu}_2 = -\left.\frac{r_2'}{r_1'}\frac{\partial\vartheta}{\partial r}\right|_{\Gamma_2}\,. \tag{8}$$

Then they were averaged on the boundaries Γ_1, Γ_2:

$$\overline{\mathrm{Nu}_1} = \frac{1}{2}\int_0^{\pi} \mathrm{Nu}_1 \sin\theta d\theta\,;\quad \overline{\mathrm{Nu}_2} = \frac{1}{2}\int_0^{\pi} \mathrm{Nu}_2 \sin\theta d\theta\,. \tag{9}$$

The averaged Nusselt numbers were tested in the mode of pure heat conduction; for this purpose the equation

$$\frac{1}{r^2}\frac{d}{dr}\left(r^2\frac{d\vartheta}{dr}\right) + Q_v = 0\,,$$

the general solution of which has the form

$$\vartheta + Q_v r^2/6 - A/r + B = 0$$

was considered. The constants A and B were determined from the corresponding boundary conditions. Then, the averaged Nusselt numbers were calculated by formulas (8) and (9). Then relations that the averaged Nusselt numbers $\overline{\mathrm{Nu}_1}$ and $\overline{\mathrm{Nu}_2}$ should satisfy were obtained by the equation of heat balance. These relations are presented in what follows:

boundary conditions of the I kind on both boundaries Γ_1, Γ_2:

$$\vartheta|_{\Gamma_1} = 1\,,\quad \vartheta|_{\Gamma_2} = 0\,,$$

$$\frac{\overline{\mathrm{Nu}_1}}{\overline{\mathrm{Nu}_2}} = \frac{\dfrac{Q_v}{3} + \dfrac{1 - \dfrac{Q_v}{6}(R_0^2 - 1)}{R_0 - 1} R_0}{\dfrac{Q_v}{3} R_0^2 + \dfrac{1 - \dfrac{Q_v}{6}(R_0^2 - 1)}{R_0 - 1}}\,,\quad R_0 = r_2'/r_1'\,, \tag{10}$$

$$\overline{\mathrm{Nu}_1} = R_0\overline{\mathrm{Nu}_2} \quad \text{at} \quad Q_v = \frac{q_v r_1'^2}{\lambda(T_1 - T_2)} = 0\,; \tag{11}$$

boundary conditions of the II and I kind:

$$-\left.\frac{\partial\vartheta}{\partial n}\right|_{\Gamma_1} = 1\,,\quad \vartheta|_{\Gamma_2} = 0\,,$$

$$\frac{\overline{\mathrm{Nu}_1}}{\overline{\mathrm{Nu}_2}} = \left[\frac{1}{R_0} - \frac{Q_v\left(\dfrac{1}{R_0} - R_0^2\right)}{3}\right]^{-1}\,,$$

$$\overline{\mathrm{Nu}_1} = R_0\,\overline{\mathrm{Nu}_2} \quad \text{at} \quad Q_v q_v r_1/q = 0\,; \tag{12}$$

boundary conditions of the I and III kind:

$$\vartheta|_{\Gamma_1} = 0\,,\quad \left.\frac{\partial\vartheta}{\partial n}\right|_{\Gamma_2} = \mathrm{Bi}_2\,(1 - \vartheta|_{\Gamma_2})\,,$$

$$\frac{\overline{\mathrm{Nu}_1}}{\overline{\mathrm{Nu}_2}} = \frac{\left[1 + \frac{Q_v}{6}\left(1 - R_0^2 - \frac{2R_0}{\mathrm{Bi}_2}\right)\right]\frac{R_0}{R_0 - 1 + 1/R_0\,\mathrm{Bi}_2} + \frac{Q_v}{3}}{\left[1 + \frac{Q_v}{6}\left(1 - R_0^2 - \frac{2R_0}{\mathrm{Bi}_2}\right)\right]\frac{1}{R_0 - 1 + 1/R_0\,\mathrm{Bi}_2} + \frac{Q_v R_0^2}{3}}, \tag{13}$$

$$\overline{\mathrm{Nu}_1} = R_0\,\overline{\mathrm{Nu}_2} \quad \text{at} \quad Q_v = \frac{q_v r_1'^2}{\lambda\,(T_1 - T_{\mathrm{liq}2})} = 0;$$

boundary conditions of the III and I kind

$$\mathrm{Bi}_1\,\vartheta|_{\Gamma_1} = \left.\frac{\partial\vartheta}{\partial n}\right|_{\Gamma_1}, \quad \vartheta|_{\Gamma_2} = 1,$$

$$\frac{\overline{\mathrm{Nu}_1}}{\overline{\mathrm{Nu}_2}} = \frac{\left[1 + \frac{Q_v}{6}\left(1 - R_0^2 - \frac{2}{\mathrm{Bi}_1}\right)\right]\frac{R_0}{(1/\mathrm{Bi}_1)\,R_0 + R_0 - 1} + \frac{Q_v}{3}}{\left[1 + \frac{Q_v}{6}\left(1 - R_0^2 - \frac{2}{\mathrm{Bi}_1}\right)\right]\frac{1}{(1/\mathrm{Bi}_1)\,R_0 + R_0 - 1} + \frac{Q_v R_0^2}{3}},$$

$$\overline{\mathrm{Nu}_1} = R_0\,\overline{\mathrm{Nu}_2} \quad \text{at} \quad Q_v = \frac{q_v r_1'^2}{\lambda\,(T_{\mathrm{liq}1} - T_2)} = 0. \tag{14}$$

The system of differential equations (5)-(7) was solved numerically by the method of control volume (the algorithm SIMPLE was used) [11].

After integration of Eqs. (5)-(7) by a control volume their discrete analogs, which were solved by the Gauss–Zeidel iteration method with lower relaxation, were obtained.

The temperature fields, stream functions, and local and averaged Nusselt numbers were found from numerical calculations. The following steady-state modes of flow and heat transfer were considered: $\mathrm{Re} = \mathrm{Pe} = 1$; $\mathrm{Gr}/\mathrm{Re}^2 = 10^3$; $\mathrm{Ra} = \mathrm{GrPr} = 10^3$ [1, 2, 4]. The ratio of the outer radius of the core r_2' to the inner r_1' varied within the range 2/1; 3/1. Results for the ratio $r_2'/r_1' = 2/1$ are given in Figs. 2-4.

Figure 2 presents calculated fields for boundary conditions of the I kind. In the core heat was transferred by heat conduction. The Rayleigh number Ra = 1000. The temperature field for all three modes ($Q_v/\mathrm{Pe} = 0, 1, 2$) makes up concentric circles crowding at the inner boundary of the core (Fig. 2a, A for $Q_v/\mathrm{Pe} = 0$, here $\overline{\mathrm{Nu}_1} > \overline{\mathrm{Nu}_2}$, the temperature distribution over the core thickness is represented by curve 1 in Fig. 2a, C) and crowding at its outer boundary for $Q_v/\mathrm{Pe} = 1, 2$ (here $\overline{\mathrm{Nu}_2} > \overline{\mathrm{Nu}_1}$, the temperature variation over the layer thickness is represented by curve 2 for $Q_v/\mathrm{Pe} = 1$ and curve 3 for $Q_v/\mathrm{Pe} = 2$ in Fig. 2a, C). Although a four-cell flow takes place in the core for all the modes (Fig. 2a, B), its intensity is virtually insignificant, and the maximum value of the stream function $|\Psi_{\max}|$ is of the order of 10^{-14}, 10^{-15}. At $Q_v/\mathrm{Pe} = 1$, $|\Psi_{\max}| = 1.44 \cdot 10^{-14}$, $\overline{\mathrm{Nu}_1} = 1.323$, $\overline{\mathrm{Nu}_2} = 1.829$, and at $Q_v/\mathrm{Pe} = 2$, $|\Psi_{\max}| = 2.23 \cdot 10^{-14}$, $\overline{\mathrm{Nu}_1} = 0.666$, $\overline{\mathrm{Nu}_2} = 2.662$. For the results in Fig. 2a, the local and averaged Nusselt numbers coincide. The latter obtained in a numerical solution of the problem, satisfy relations (11), (10) for the corressponding modes ($Q_v = 0$ and $Q_v \neq 0$) with an absolute error of 10^{-2}.

Figure 2b presents calculated fields for the Rayleigh number Ra = 3000 in the absence of an internal heat source. As is seen from the figure, in this mode heat is transferred by convection. The temperature field in the layer and the temperature distribution over the layer thickness acquire a pronounced character for developed convection. The intensity of motion and heat transfer increases; this is indicated by the increase in the stream function ($|\Psi_{\max}| = 3.29$) and the averaged Nusselt numbers ($\overline{\mathrm{Nu}_1} = 2.924$; $\overline{\mathrm{Nu}_2} = 1.478$). Thermal boundary layers

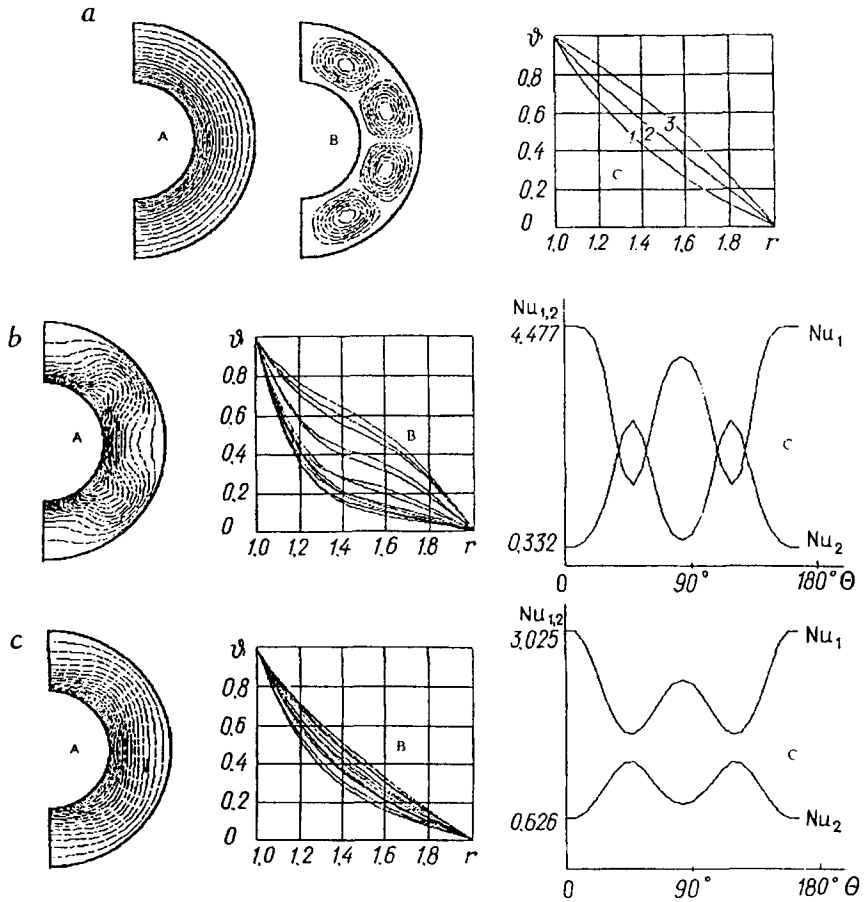

Fig. 2. Calculated fields (boundary conditions of the I kind): a) A, temperature field; B, stream function; C, temperature distribution over the core thickness; the parameters: Ra = 1000, $|\Psi_{max}| = 6.60 \cdot 10^{-15}$, $\overline{Nu_1} = 1.979$, $\overline{Nu_2} = 0.996$; b) A, B, field and distribution of the temperature over the core thickness; C, distribution of the local Nusselt numbers on the inner and outer boundaries of the core as a function of the latitude; the parameters: 3000, 3.29, 2.924, 1.478; c) A, B, field and distribution of the temperature over the core thickness; C, distribution of the local Nusselt numbers on the inner and outer boundaries as a function of the latitude; the parameters: 2300, 0.78, 2.096, 1.060.

are formed on the inner and outer surfaces of the core. The variation of the local Nusselt numbers has a "wave" character with a symmetry relative to the angle $\Theta = 90^0$ (Fig. 2b, C). The flow pattern in the layer is similar to that in the above-considered modes (Fig. 2a, B). It is known [8] that the value of the critical Rayleigh number Ra^* corresponding to the stability region is proportional to the first eigenvalue of the considered boundary-value problem and can be found numerically directly from its differential formulation. By virtue of this, numerical calculations, which allowed the determination of $Ra^* \sim 2000$, were performed in order to find the critical Rayleigh number. The critical number found should be assumed to represent the lower level of the instability spectrum characterizing the onset of convection in the layer. We note that for a plane horizontal layer with solid boundaries the minimum critical Rayleigh number at the basic level of instability is $Ra^* = 1707.762$ [6]. The difference in the values of the critical numbers is likely associated with the curvature of the considered region.

Figure 2c presents results of calculations for Ra = 2300 that indicate that at $Ra > Ra^* = 2000$ a convective mechanism of energy transfer begins to develop in the layer. The temperature field already differs from concentric circles (Fig. 2c, A), stratification of the temperature over the core thickness is observed (Fig. 2c, B), and the change

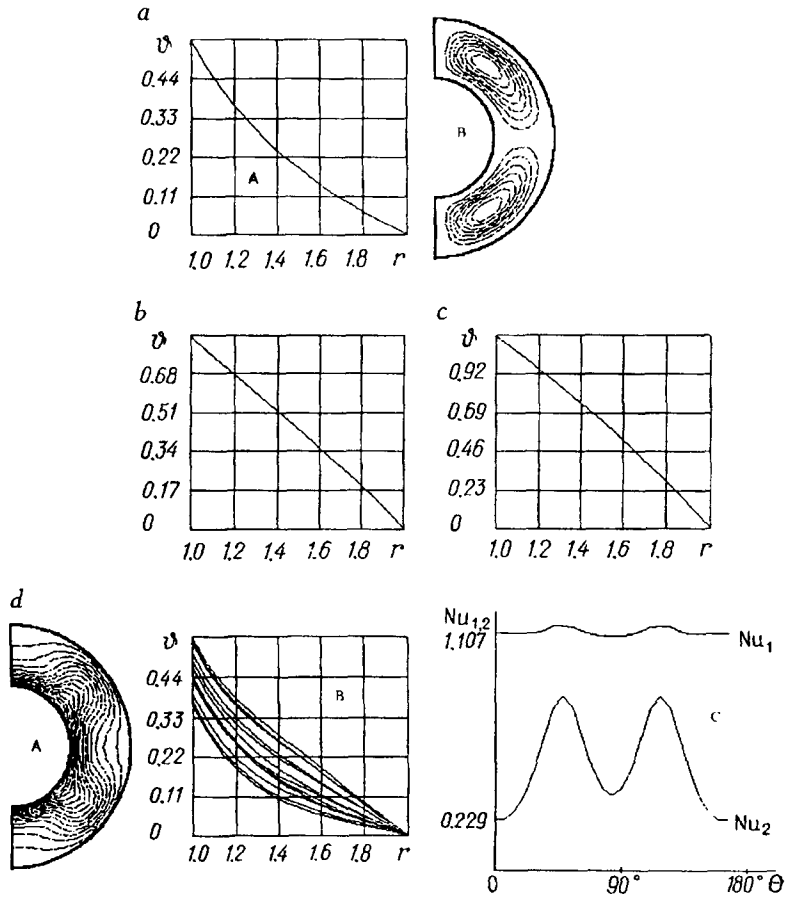

Fig. 3. Calculated fields (boundary conditions of the II kind): a) A, temperature field; B, stream function; the parameters: Ra = 1000, Q_v/Pe = 0, $|\Psi_{max}| = 3.30 \cdot 10^{-12}$, $\overline{Nu_1} = 1.061$, $\overline{Nu_2} = 0.534$; b) temperature distribution over the core thickness; the parameters: 1000, 1, $4.10 \cdot 10^{-12}$, 1.061, 0.534; c) same; the parameters: 1000, 2, $1.43 \cdot 10^{-11}$, 0.994, 2.8828; d) A, B, field and distribution of the temperature over the core thickness; c, distribution of the local Nusselt numbers on the inner and outer boundaries of the core as a function of the latitude; the parameters: 4000, 0, 1.188, 1.079, 0.544.

in the local Nusselt numbers has a "wavy" character, but for this mode (unlike the results of Fig. 2b, B) the curves of Nu_1 and Nu_2 do not intersect.

Results of a calculation for the case of boundary conditions of the II kind

$$\left.\frac{\partial \vartheta}{\partial n}\right|_{r_1} = -1, \quad \vartheta|_{r_2} = 0$$

are presented in Fig. 3, where it is seen that heat is transferred by heat conduction, and therefore, the local and averaged Nusselt numbers coincide. The temperature on the inner boundary of the core increases with increase in the internal heat flux Q_v (this is indicated by a comparison of the temperature variation in the core in Figs. 3a, A, 3b, and 3c). As in the case of boundary conditions of the I kind, the temperature field is represented by concentric circles, similar to those in Fig. 2a, A, that crowd at the inner boundary for $Q_v = 0$ ($\overline{Nu_1} > \overline{Nu_2}$) and at the outer boundary for $Q_v \neq 0$ ($\overline{Nu_2} > \overline{Nu_1}$). The rate of convection is small, and a two-vortex flow takes place in all cases (Fig. 3a, B). Compared to the results given in Fig. 2a, B, here the rate of convection is higher: $|\Psi_{max}| \sim 10^{-11}$. The calculated averaged Nusselt numbers satisfy relations (11), (12) with an absolute error of 10^{-2}. The critical value of the Rayleigh number $Ra^* \sim 3300$ is found numerically for the given type of boundary conditions and $Q_v =$

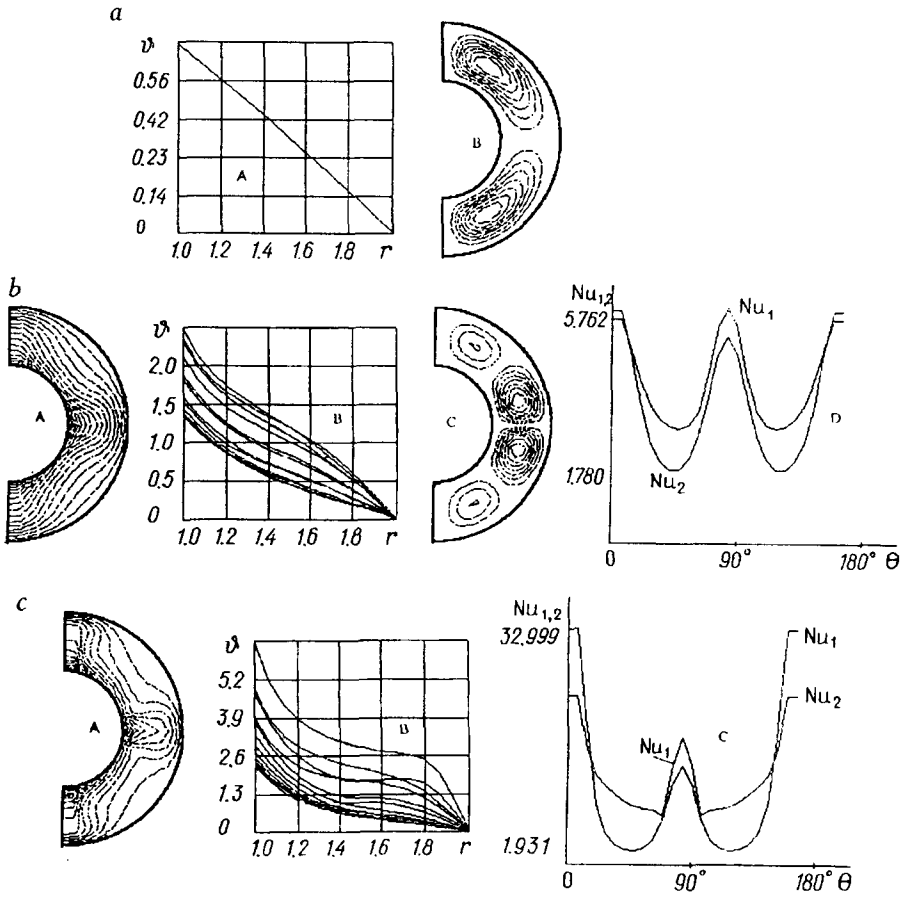

Fig. 4. Calculated fields (boundary conditions of the III kind): a) A, temperature distribution over the core thickness; B, stream function; the parameters: $|\Psi_{max}| = 2.93 \cdot 10^{-14}$, $\overline{Nu}_1 = 0.686$, $\overline{Nu}_2 = 1.509$; b) A, B, field and distribution of the temperature over the core thickness; C, stream function; D, distribution of the local Nusselt numbers on the inner and outer boundaries of the core as a function of the latitude; the parameters: 2.12, 3.762, 3.026; c) A, B, field and distribution of the temperature over the core thickness; C, distribution of the local Nusselt numbers on the inner and outer boundaries of the core as a function of the latitude; the parameters: 4.47, 10.413, 6.378.

0. The values of the averaged Nusselt numbers are the same as for the version presented in Fig. 2a, the rate of convection is $|\Psi_{max}| \sim 10^{-8}$, and the flow becomes four-cell as in Fig. 2a, B. Figure 3d shows results for $Q_v = 0$, $Ra = 4000 > Ra^*$. In the core a convective mechanism of energy transfer dominates. The temperature field differs from concentric circles (Fig. 3d, A), temperature stratification takes place over the core thickness (Fig. 3d, B), and thermal boundary layers form on the boundaries of the core. The change in the local Nusselt numbers (especially on the outer boundary) has a "wavy" character. Four vortices with a rate $|\Psi_{max}| = 1.188$ occur in the layer (as in Fig. 2a, B). The numerically calculated averaged Nussselt numbers exceed the corresponding values calculated by formula (12) for the mode of heat conduction.

Results obtained for boundary conditions of the III kind on the surface of the core

$$\left.\frac{\partial \vartheta}{\partial n}\right|_{\Gamma_1} = -\vartheta|_{\Gamma_1} \quad \text{(Fig. 4, } a\text{)}, \qquad \left.\frac{\partial \vartheta}{\partial n}\right|_{\Gamma_1} = -2\vartheta|_{\Gamma_1} \quad \text{(Fig. 4, } b\text{)};$$

$$\left.\frac{\partial \vartheta}{\partial n}\right|_{\Gamma_1} = -3\vartheta|_{\Gamma_1} \quad \text{(Fig. 4, } c\text{)};$$

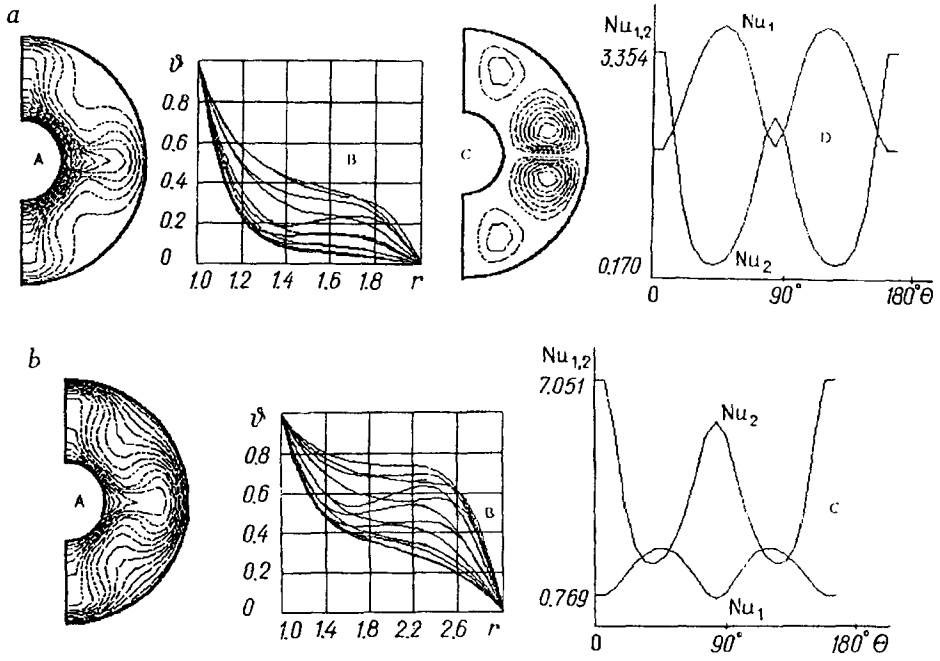

Fig. 5. Calculated fields (boundary conditions of the I kind): a) A, B, field and distribution of the temperature over the core thickness; C, stream function; D, distribution of the local Nusselt numbers on the inner and outer boundaries of the core as a function of the latitude; the parameters: $Q_v/\mathrm{Pe} = 0$, $|\Psi_{max}| = 8.64$, $\overline{Nu}_1 = 2.740$, $\overline{Nu}_2 = 0.922$; b) A, B, field and distribution of the temperature over the core thickness; C, distribution of the local Nusselt numbers on the inner and outer boundaries of the core as a function of the latitude; the parameters: 1, 11.22, 1.624, 3.476.

are shown in Fig. 4 (on the outer boundary of the core the temperature was maintained equal to zero, $\vartheta|_{\Gamma_2} = 0$). Internal heat sources ($Q_v/\mathrm{Pe} = 1$) occur for all cases.

For the results of Fig. 4a, energy in the layer is transferred by heat conduction. The temperature field is concentric circles as in Fig. 2a, A. The distribution of the temperature over the thickness of the spherical layer is presented in Fig. 4a, A. Two vortices of small intensity $|\Psi_{max}| \sim 10^{-14}$ occur in the layer (Fig. 4a, B). With increase in the amount of heat supplied from below, heat in the layer is transferred by convection, and rearrangement of the temperature field, particularly pronounced in the region of $\Theta \sim 0$, 90, 180°, takes place (Figs. 4b, A and 4c, A). On the inner surface of the core the temperature increases with increase in the Biot number Bi_1, and the distribution of the temperature over the layer thickness acquires a form typical of convective transfer of energy (Figs. 4b, B and 4c, B). For the modes whose results are presented in Fig. 4b, c, an intense four-cell flow occurs in the region studied (Fig. 4b, B).

For the mode of Fig. 4a the local and averaged Nusselt numbers coincide. Figure 4b, D ($Bi_1 = 2$) shows the change in the local Nusselt numbers, which has a "wavy" character; the curves of $\overline{Nu}_1$ and $\overline{Nu}_2$ differ slightly but still do not intersect. A further increase in the power of the heat flux supplied from inside ($Bi_1 = 3$, Fig. 4c) increases the rate of convection $|\Psi_{max}| \sim 4$, and rearrangement of the temperature field in the layer persists, thus leading to an increase in the Nusselt numbers. The curves of $\overline{Nu}_1$, $\overline{Nu}_2$ (Fig. 4c, B) have common points characterized by equality of the local heat fluxes. The ratio of the Nusselt numbers calculated by formula (14) differs 2-4-fold from the corresponding value calculated by relation (9) (for the results of Fig. 4b, c). This fact confirms that heat in the core is transferred by convection, and heat conduction is small.

Results for the ratio $r_2'/r_1' = 3/1$ are presented in Figs. 5-7. Fields calculated for boundary conditions of the I kind are shown in Fig. 5. In the core, energy is transferred by convection; this can be judged by the change in the field characteristic of convective heat transfer and the distribution of the temperature (Fig. 5a, A, B and Fig.

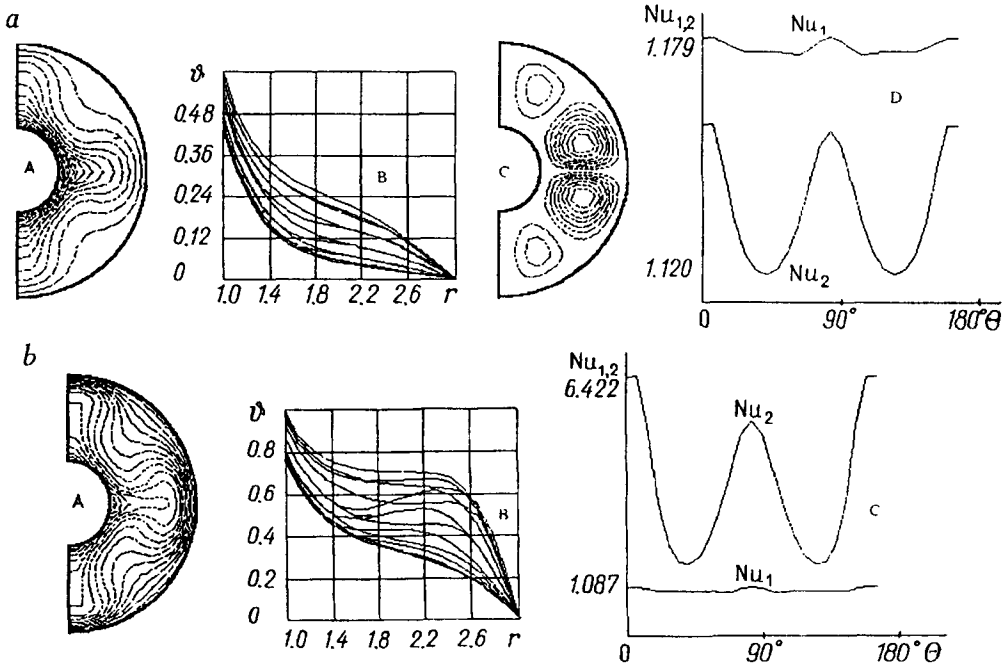

Fig. 6. Calculated fields (boundary conditions of the II kind): a) A, B, field and distribution of the temperature over the core thickness; C, stream function; D, distribution of the local Nusselt numbers on the inner and outer boundaries of the core as a function of the latitude; the parameters: $Q_v/\mathrm{Pe} = 0$, $|\Psi_{max}| = 4.67$, $\overline{Nu_1} = 1.128$, $\overline{Nu_2} = 0.377$; b) A, B, field and distribution of the temperature over the core thickness; C, distribution of the local Nusselt numbers on the inner and outer boundaries of the core as a function of the latitude; the parameters: 1, 10.30, 1.116, 3.292.

5b, A, B). The intensity of motion and the heat transfer increase when internal sources occur in the core: $|\Psi_{max}| \sim 8$ at $Q_v = 0$, $|\Psi_{max}| \sim 11$ at $Q_v = 1$. The presence of internal heat sources increases the gradients of the temperature at the outer boundary of the core (Fig. 5b, A) compared to the result shown in Fig. 5a, A ($Q_v = 0$), thus leading to an increase in the Nusselt numbers on the outer surface. The temperature stratification over the layer thickness becomes more pronounced for $Q_v = 1$ (Fig. 5b, B). The change in the Nusselt numbers has a "wavy" character (Fig. 5a, D and Fig. 5b, C). A developed four-cell flow occurs for the modes considered (Fig. 5a, C), with the vortices in the region of $\Theta \sim 90^\circ$ being more intense than at the poles $\Theta \sim 0, 180^\circ$. The critical Rayleigh number for $Q_v = 0$ obtained as a result of a numerical experiment amounts to $Ra^* \sim 300$. The temperature field for this mode is concentric circles. The entire flow region is occupied by two votrtices of low intensity $|\Psi_{max}| \sim 10^{-4}$. The local Nusselt numbers coincide with the averaged ones, and in this case $\overline{Nu_1} = 1.465$, $\overline{Nu_2} = 0.498$. The calculation made by Sherman, which refines the value of the lower critical Rayleigh number and is given in [6] for the particular case of a spherical cavity (not a layer as in this paper) with an ideally conducting boundary, yielded the critical Rayleigh number $Ra^* = 745.9$. The same paper ([6], Table 7) gives the critical Rayleigh number for a horizontal cylinder with an ideally conducting boundary $Ra^* = 408.2$. Table 4 of [6] drawn up for some variants of the boundary conditions (unfortunately, none suits for comparison with the results of the present paper) presents critical values Ra^* of the horizontal layer that range from 120 to 816.4. An analysis and comparison of the order of the values of the critical Rayleigh numbers Ra^* calculated and given in [6] make it possible to verify that the numerical algorithm and the results obtained are correct.

Temperature fields, stream functions, and local Nusselt numbers calculated for boundary conditions of the II kind

$$\left.\frac{\partial \vartheta}{\partial n}\right|_{\Gamma_1} = -1, \quad \vartheta|_{\Gamma_2} = 0,$$

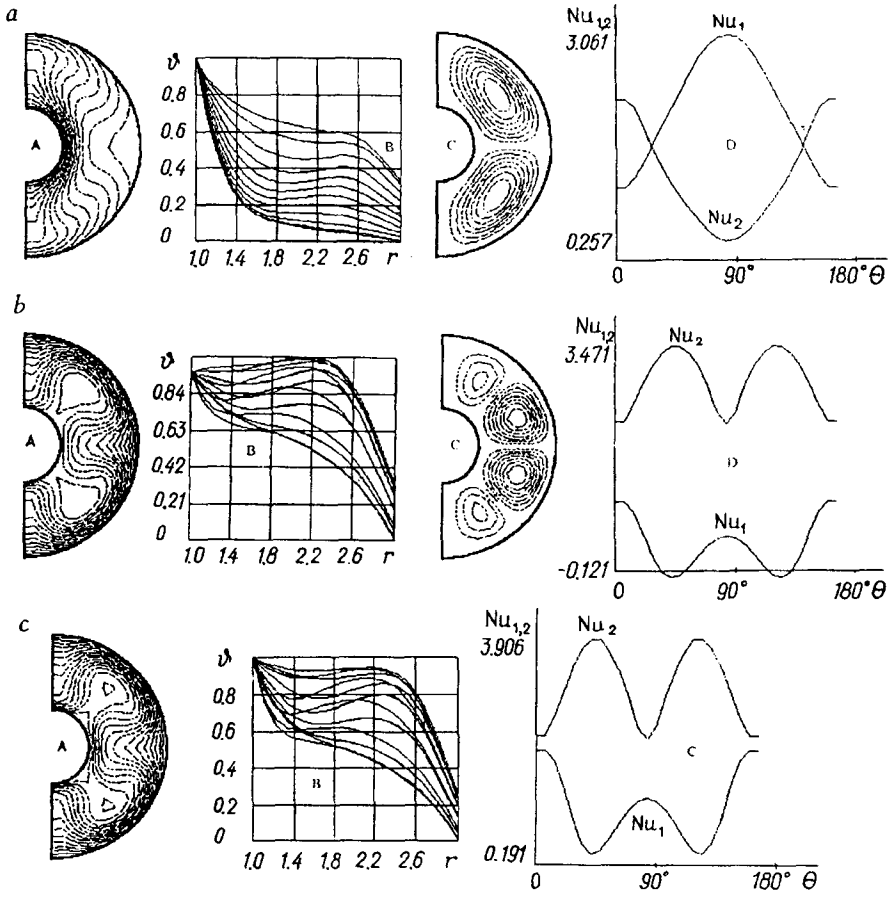

Fig. 7. Calculated fields (boundary conditions of the III kind): a) $Q_v/\mathrm{Pe} = 0$, $|\Psi_{max}| = 7.30$, $\overline{Nu_1} = 2.394$, $\overline{Nu_2} = 0.815$; b) 1, 8.65, 0.254, 3.018, respectively; A, B, field and distribution of the temperature over the core thickness; C, stream function; D, distribution of the local Nusselt numbers on the inner and outer boundaries of the core as a function of the latitude; c) A, B, field and distribution of the temperature over the core thickness; C, distribution of the local Nusselt numbers on the inner and outer boundaries of the core as a function of the latitude; the parameters: 1, 9.46, 0.765, 3.200.

are depicted in Fig. 6. As in the case of boundary conditions of the I kind, natural-convection heat transfer with a temperature profile characteristic of this mechanism of energy transfer occurs here (Fig. 6a, A, B and Fig. 6b, A, B). The presence of an internal heat source in the layer increases temperature stratification (Fig. 6b, B) compared to the result shown in Fig. 6a, B ($Q_v = 0$). The local Nusselt numbers (Fig. 6a, D and Fig. 6b, C) on the inner boundary of the core virtually do not change, taking on a "wavy" character on the outer surface. At $Q_v = 0$ the local heat flux Nu_1 on the inner boundary (Fig. 6a, D) exceeds the local heat flux Nu_2 on the outer boundary. The picture changes to the opposite at $Q_v = 1$ (Fig. 6b, C): the local heat flux decreases on the inner boundary and increases on the outer. In the liquid core in both the presence and the absence of an internal heat source four vortices are formed: intense ones near the equatorial plane and small at the poles (Fig. 6a, C). As in the previous case, the critical Rayleigh number is $Ra^* \sim 300$ for $Q_v = 0$. The temperature field is concentric circles. The flow pattern is represented by two vortices of low intensity $|\Psi_{max}| \sim 10^{-4}$. The local heat fluxes coincide with the averaged: $\overline{Nu_1} = 1.093$ and $\overline{Nu_2} = 0.371$.

Figure 7 shows calculated fields for boundary conditions of the III kind on the outer surface of the core:

$$\left.\frac{\partial\vartheta}{\partial n}\right|_{\Gamma_2} = -2\vartheta|_{\Gamma_2} \quad \text{(Fig. 7, } a \text{ and } b\text{)}, \qquad \left.\frac{\partial\vartheta}{\partial n}\right|_{\Gamma_2} = -3\vartheta|_{\Gamma_2} \quad \text{(Fig. 7, } c\text{)}.$$

On the inner surface of the core $\vartheta|_{\Gamma_1} = 0$.

For the results presented in Fig. 7a heat is transferred by convection. The temperature field and the temperature distribution over the core thickness, typical of convective heat transfer, are shown in Fig. 7a, A and B. As is seen from Fig. 7a, A, on the outer boundary of the core the temperature increases at the poles ($\Theta = 0$, 180^0) and decreases at the equator ($\Theta = 90^0$). Two vortices are formed in the liquid core (Fig. 7a, B); in the presence of internal heat sources (Fig. 7b and c) these vortices are transformed into four vortices (Fig. 7b, B). In this case the character of the variation of the fields of the temperature (Fig. 7b, A and Fig. 7c, A), the stream function (Fig. 7b, C), and the Nusselt numbers (Fig. 7b, D and Fig. 7b, C) becomes different from the corresponding fields presented in Fig. 7a.

The averaged Nusselt numbers for the modes given in Figs. 5a, B; 6a, C; 7a, D, obtained in the numerical solution of the problem, satisfy relation (11) with an absolute error of $(2-5)\cdot 10^{-2}$, and for the results shown in Figs. 5b, B; 6b, B; 7b, D, and 7c, C the values calculated by formulas (10), (12), and (13) differ from the corresponding values obtained by relation (9). Hence it follows that developed convection takes place in the core; this is confirmed by the results presented in Figs. 5b, 6b, 7b, and 7c. The critical Rayleigh number $Ra^* \sim 250$ is calculated for $Q_v = 0$. In this case in the computational region two vortices with a maximum value of the stream function $|\Psi_{max}| \sim 1.057\cdot 10^{-12}$ are formed, and the averaged Nusselt numbers take the values $\overline{Nu}_1 = 1.348$ and $\overline{Nu}_2 = 0.458$.

Thus, an analysis of the results obtained allows one to draw the following conclusions.

1. The presence of internal heat sources increases the rate of heat transfer and motion of the liquid in the earth core. The gradients of the temperature on the outer boundary increase compared to the gradients on the inner surface (at $Q_v = 0$ the tendency is opposite).

2. At the ratio $r_2'/r_1' = 2/1$ and $Ra = 1000$ heat in the layer is transferred by heat conduction. The intensity of convection is small. In the case of boundary conditions of the I kind a four-cell flow occurs in the layer, and this flow is transformed to two-cell in the case of heat supply from below.

3. At the ratio $r_2'/r_1' = 3/1$ and $Ra = 1000$ developed convection exists in the liquid core, and the flow pattern is represented by four vortices, except for the mode shown in Fig. 7a.

4. For different versions of the boundary conditions and the thickness of the layers critical Rayleigh numbers are calculated, which allowed determination of the lower level characterizing the onset of convection in the spherical layer.

5. The model suggested and the results obtained complement the available information on the motions of the liquid inside the earth core, and this can serve as a guiding line for the study of more realistic processes, which in all cases require bulky numerical calculations.

NOTATION

P_0, ρ_0, u_0, t_0, characteristic scales of pressure, density, velocity, and time; T, T_1, T_2, dimensional current temperature and temperature on the inner and outer surfaces of the core, respectively; β, coefficient of thermal expansion; ν, kinematic viscosity; q, density of the heat flux supplied to the inner boundary of the core; Nu_1, Nu_2, $\overline{Nu}_1$, $\overline{Nu}_2$, local and averaged Nusselt numbers on the inner (Γ_1) and outer (Γ_2) surfaces of the core, respectively; Ra^*, critical Rayleigh number; n, normal to the surface of the core; R_0, dimensionless outer radius of the core; Ψ_{max}, maximum value of the stream function in the earth core. Subscripts: 0, undisturbed values; 1, inner surface; 2, outer surface; liq, liquid; max, maximum value; ν, volume.

REFERENCES

1. B. M. Yankovskii, The Earth's Magnetism [in Russian], Leningrad (1978).
2. V. N. Zharkov, V. P. Trubitsyn, and L. V. Samsonenko, Physics of the Earth and the Planets. Figures and Interior Structure [in Russian], Moscow (1991).

3. F. Krause and K.-H. Radler, Magnetic Hydrodynamics of Mean Fields and Dynamo Theory [Russian translation], Mosocw (1984).
4. V. N. Zharkov, Interior of the Earth and the Planets [in Russian], Moscow (1983).
5. O. G. Martynenko and Yu. A. Sokovishin, Free-Convection Heat Transfer: Reference Book [in Russian], Minsk (1982).
6. G. Z. Gershuni and E. M. Zhukhovitskii, Convective Stability of an Incompressible Liquid [in Russian], Moscow (1972).
7. L. D. Landau and E. M. Lifshits, Hydrodynamics [in Russian], Moscow (1988).
8. V. G. Babskii, N. D. Kopachevskii, and A. D. Myshkis, Hydromechanics of Weightlessness (ed. A. D. Myshkis) [in Russian], Moscow (1976).
9. Yu. A. Sokovishin and O. G. Martynenko, Introduction to the Theory of Free-Convection Heat Transfer [in Russian], Leningrad (1982).
10. A. D. Gosman, V. M. Pan, A. K. Ranchel, D. B. Spalding, and M. Volfstein, Numerical Methods of the Study of Viscous-Fluid Flows [Russian translation], Moscow (1972).
11. S. Patankar, Numerical Methods of Solution of Problems of Heat Transfer and Fluid Dynamics [Russian translation], Moscow (1984).